4th Specialty Conference on Coastal, Estuary and Offshore Engineering
*4e Conférence spécialisée sur l'ingénierie côtière et en milieu maritime*

Montréal, Québec
May 29 to June 1, 2013 / *29 mai au 1 juin 2013*

# Numerical Simulation of Thermal Buoyant Wall Jets

H. Kheirkhah Gildeh[1], A. Mohammadian[2], I. Nistor[3], H. Qiblawey[4]
[1,2,3]Department of Civil Engineering, University of Ottawa
[4]Department of Chemical Engineering, University of Qatar

**Abstract:** The main focus of this study is on the near field flow and mixing characteristics of the thermal wall jets. A numerical study of the buoyant wall jets discharged from submerged outfalls from cooling systems of power plants has hence been conducted. The effects of different RANS (Reynolds-Averaged Navier-Stokes) turbulence models have been investigated. The standard k-ε, RNG k-ε, realizable k-ε and SST k-ω turbulence models have been applied in this study. A finite volume method with structured grid was used to simulate the flow and temperature fields. The results of temperature and velocity fields are compared to both existing experimental and numerical data. It is found that the realizable k-ε performs the best among the four investigated turbulence models. According to the results from different simulations, relationships and comparative graphs are presented which are helpful for a better understanding of buoyant wall jets.

## 1 Introduction

When a buoyant jet is discharged into a marine environment, at a point remote from any boundary of the domain considered, it rises and mixes with the ambient fluid because of the turbulent flow generated by the presence of shear stresses that develop around the jet-ambient liquid interface. Nevertheless, if the effluent is discharged in touch with a solid horizontal boundary, it is subjected to the Coanda effect and clings to the floor for a while before the effect of buoyancy forces, which cause the jet to lift and rise away from this horizontal boundary (e.g. Foster and Parker, 1970) as shown in Figure 1. Such a buoyant wall jet, is widely used in practice due to the ease of outfall construction, and has been extensively studied in the literature (e.g. Anwar, 1969).

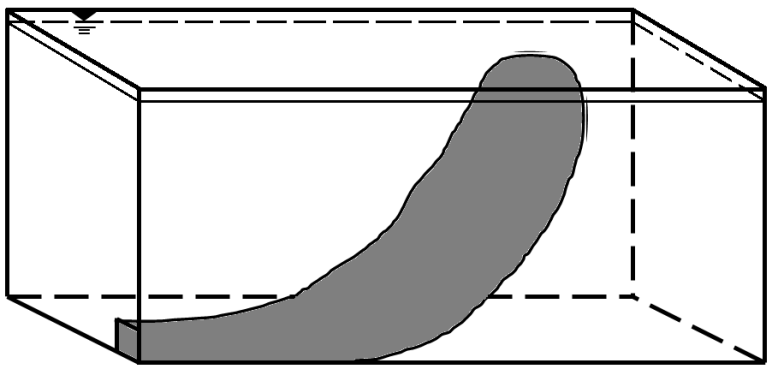

Figure 1: A buoyant wall jet discharge.

A large number of studies have been performed on buoyant jets (e.g. Sforza and Herbst, 1970; Rajaratnam and Pani, 1974; Balasubramanian and Jain, 1978 and Kuang and Lee, 2002). Sharp (1975, 1977) is one of the pioneers who considered submerged outfall of thermal effluents as a buoyant wall jet. His study focused on the properties of a buoyant jet discharged immediately above a horizontal surface. The jet behaved as a wall jet in the initial part of its trajectory; nonetheless after rising from the surface to which it initially clung, the jet acted as a normal free jet. Sobey et al. (1988) studied buoyant discharge in perhaps its most elementary geometry - a round buoyant jet discharging horizontally from a vertical side wall into a stationary water body on a flat-bed. Law and Herlina (2002) applied novel experimental equipment, a combination of Particle Image Velocimetry (PIV) and Plannar Laser Induced Fluorescence (PLIF) approach, in order to study a circular three-dimensional turbulent wall jet. More recently, Michas and Papanicolaou (2008) investigated horizontal, round turbulent buoyant jets that discharge into a homogeneous, calm ambient fluid.

All of the above-mentioned studies were conducted experimentally. However, numerical simulations on buoyant wall jets are still being studied and require further investigation. Maele and Merci (2006) applied standard and realizable k-ε turbulence models and examined different types of buoyant plumes. They found out that the realizable k-ε model performs better for the cases considered. Kim and Cho (2006) investigated buoyant flow of heated water discharged from surface and submerged side outfalls in shallow and deep water with a cross flow. They used the FLOW-3D which is a commercial CFD (Computational Fluid Dynamics) package and RNG k-ε model was applied for turbulence closure. Xiao et al. (2009) developed a fast non-Boussinesq integral model for the horizontal turbulent buoyant jets by using a CFD code named GASFLOW. Based on Sharps' experimental data (1975, 1977), recently, Huai et al. (2010) investigated horizontal buoyant wall jet numerically. They only applied one turbulence model, realizable k-ε, for their study. They presented results mainly for the near field and proposed some relationships between the distance and the dilution of velocity and temperature based on the numerical results.

## 2 Mathematical Concepts

### 2.1 Governing Equations

The governing equations are the well-known Navier-Stokes equations for three-dimensional incompressible fluids as follows:

Continuity Equation:

[1] $$\frac{\partial u}{\partial x}+\frac{\partial v}{\partial y}+\frac{\partial w}{\partial z}=0$$

Momentum Equations:

[2] $$\frac{\partial u}{\partial t}+u\frac{\partial u}{\partial x}+v\frac{\partial u}{\partial y}+w\frac{\partial u}{\partial z}=-\frac{1}{\rho}\frac{\partial P}{\partial x}+\frac{\partial}{\partial x}\left(\upsilon_{eff}\left(\frac{\partial u}{\partial x}\right)\right)+\frac{\partial}{\partial y}\left(\upsilon_{eff}\left(\frac{\partial u}{\partial y}\right)\right)+\frac{\partial}{\partial z}\left(\upsilon_{eff}\left(\frac{\partial u}{\partial z}\right)\right)$$

[3] $$\frac{\partial v}{\partial t}+u\frac{\partial v}{\partial x}+v\frac{\partial v}{\partial y}+w\frac{\partial v}{\partial z}=-\frac{1}{\rho}\frac{\partial P}{\partial y}+\frac{\partial}{\partial x}\left(\upsilon_{eff}\left(\frac{\partial v}{\partial x}\right)\right)+\frac{\partial}{\partial y}\left(\upsilon_{eff}\left(\frac{\partial v}{\partial y}\right)\right)+\frac{\partial}{\partial z}\left(\upsilon_{eff}\left(\frac{\partial v}{\partial z}\right)\right)-g\frac{\rho-\rho_0}{\rho}$$

[4] $$\frac{\partial w}{\partial t}+u\frac{\partial w}{\partial x}+v\frac{\partial w}{\partial y}+w\frac{\partial w}{\partial z}=-\frac{1}{\rho}\frac{\partial P}{\partial z}+\frac{\partial}{\partial x}\left(\upsilon_{eff}\left(\frac{\partial w}{\partial x}\right)\right)+\frac{\partial}{\partial y}\left(\upsilon_{eff}\left(\frac{\partial w}{\partial y}\right)\right)+\frac{\partial}{\partial z}\left(\upsilon_{eff}\left(\frac{\partial w}{\partial z}\right)\right)$$

where *u, v, w* are the mean velocity components in the *x, y, z* direction, respectively, *t* is the time, *P* is the fluid pressure, $\upsilon_{eff}$ represents the effective kinematic viscosity ($\upsilon_{eff} = \upsilon_t + \upsilon$), $\upsilon_t$ is the turbulent kinematic viscosity, *g* is the gravity acceleration, $\rho$ is the fluid density, and $\rho_0$ is the reference fluid density.
One should note that the equations are divided by density ($\rho$) and the buoyancy term is added to the momentum equation in vertical direction (*y*-coordinate) to account for variable density effects.
Temperature evolution is modeled using the advection-diffusion equation as:

$$[5] \quad \frac{\partial T}{\partial t} + u\frac{\partial T}{\partial x} + v\frac{\partial T}{\partial y} + w\frac{\partial T}{\partial z} = k_{eff}\left(\frac{\partial^2 T}{\partial x^2} + \frac{\partial^2 T}{\partial y^2} + \frac{\partial^2 T}{\partial y^2}\right)$$

with

$$[6] \quad k_{eff} = \frac{\upsilon_t}{\mathrm{Pr}_t} + \frac{\upsilon}{\mathrm{Pr}}$$

where *T* is the fluid temperature, $k_{eff}$ is the heat transfer coefficient, *Pr* is the Prandtl number, and $Pr_t$ is the turbulent Prandtl number. In the present study, it was numerically found that the results are not significantly sensitive to $Pr_t$ and *Pr* within the range of (0.6-1). Thus, both coefficients were set to 1.0.

### 2.2 Boundary Conditions

The sketch of the numerical model is shown in Figure 2 with its coordinate system.

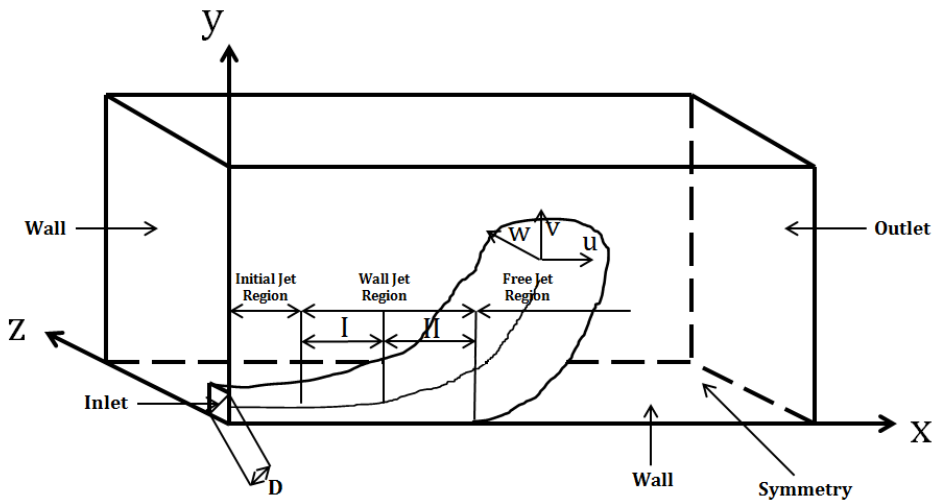


Figure 2: Schematic view of the model and coordinate system.

Only half of the wall jet domain is considered in this study due to the symmetry of the problem. The dimensions of the computational domain are chosen based on the available experimental setups. The numerical simulations were performed in a tank with dimensions of 2 m length, 0.4 m width, and 1.2 m depth (Figure 3a). A refined mesh is used for all simulations to better capture velocity and temperature characteristics in the near field zone (Figure 3b).

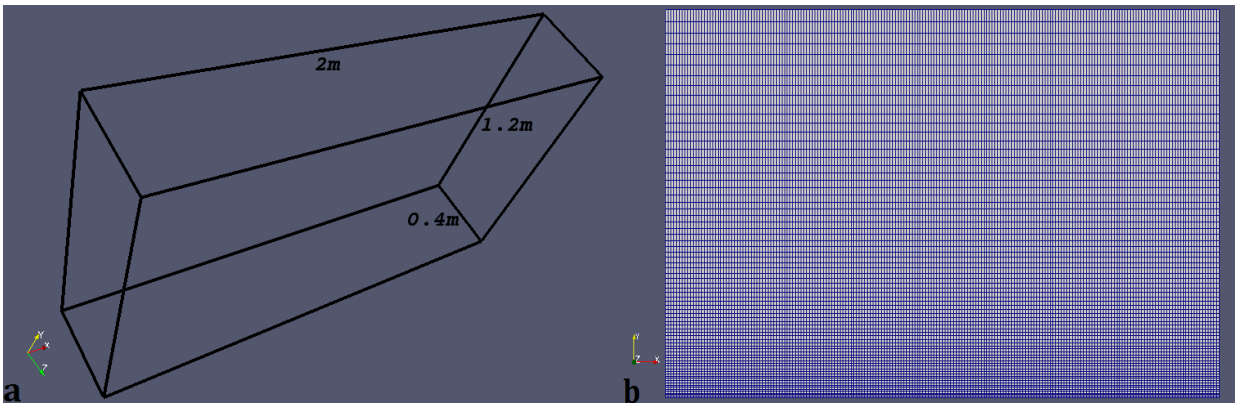


Figure 3: Computational domain. (a) Domain dimensions of numerical model. (b) A refined mesh system.

For the inlet, as shown in Figure 2, the boundary conditions are: $u=U_0$, $v=w=0$, $T=T_0$, $k=0.06u^2$, $\varepsilon=0.06u^3/D$, $\omega=\varepsilon/k$. The inlet values for $k$ and $\varepsilon$ are chosen based on Huai et al. (2010). Regarding the flow at the outlet section, a zero gradient boundary condition perpendicular to the outlet plane is defined for $u$, $v$, $w$, $k$, $\varepsilon$, $\omega$ and $T$. Moreover, for the wall boundaries, the standard wall functions are used for $k$, $\varepsilon$ and $\omega$ and the no-slip condition is considered. Finally, the symmetry boundary was modeled using zero gradient conditions.

## 3 Turbulence Models

It is widely accepted among researchers in the field that no single turbulence model can be universally applied to all situations. Some considerations must be taken into account when choosing a turbulence model including: the physics encompassed in the flow, the level of accuracy and the computational resources available. In order to evaluate the performance of different turbulence models for buoyant jet discharges, four turbulence models are considered in this paper including (i) standard k-ε model, (ii) RNG (Re-Normalization Group) k-ε model, (iii) realizable k-ε model and (iv) Shear Stress Transport (SST) k-ω model.
The OpenFOAM (**OPEN F**ield **O**peration **A**nd **M**anipulation) CFD model which is a free, and open-source software package produced by OpenCFD Ltd (2011), was used in simulations.

## 4 Results and Discussion

### 4.1 Cling Length and Trajectory

As the fluid leaves the inlet which is attached to the horizontal wall, water entrainment occurs from all directions to the jet except for the wall region. This causes a lower pressure on the wall than at the top of the jet. This keeps the jet on the wall up to a point where the top suction pressure decreases and the buoyancy force becomes larger than the pressure difference. Therefore, the wall buoyant jets can be divided in three regions: (i) Initial Jet Region, (ii) Wall Jet Region, and (iii) Free Jet Region. The Initial Jet Region is the distance from the inlet to the point where the velocity profile is almost uniform and equal to the maximum initial velocity. The Wall Jet Region itself is divided into two regions as explained in the following. The first region is the Wall Jet Region I which spans from the end of Initial Jet Region to the point where the jet centerline leaves the horizontal level and starts rising. Wall jet region II spans from the latter point to the point where the outer layer of jet leaves the floor. The Free Jet Region starts after the Wall Jet Region. These regions are shown in Figure 2.
Cling length is often defined as the distance between the inlet and the position where the floor (wall) temperature has the condition of $(T-T_a)/(T_0-T_a)=3\%$ (e.g. Huai et al., 2010). The numerical results obtained for the cling length are presented in Figure 4 and are compared with experimental and other numerical results. The axes are dimensionless and $x$ axis represents the densimetric Froude number.

The results show good agreement with both the experimental and other researchers' numerical data. However, results show that for higher Froude numbers, the experimental cling length values obtained by Sharp (1977) are smaller than the numerical results published by Huai et al. (2010), and are more

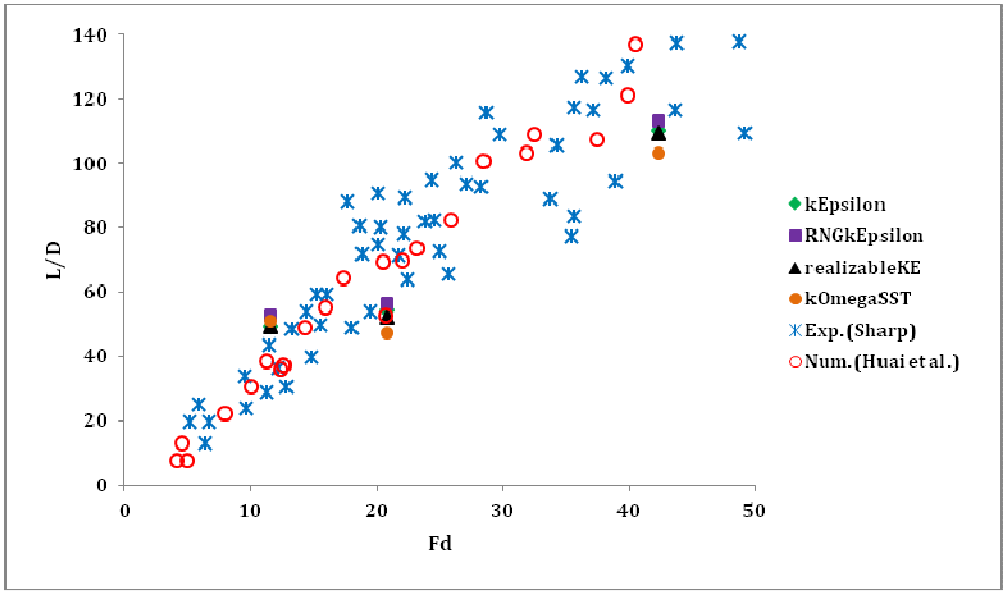


Figure 4 : Comparison of experimental and numerical values of the cling length.

consistent with the numerical results obtained in present study. The relationship between *L/D* and $F_d$ for each turbulence model is given in Table 1. Sharp (1977) suggested the same relationship, $L/D=3.2F_d$.

Table 1: Cling length relationship according to the turbulence model used.

| Turbulence Model | kEpsilon | RNGkEpsilon | realizableKE | kOmegaSST |
|---|---|---|---|---|
| Cling Length | $L/D=2.70F_d$ | $L/D=2.90F_d$ | $L/D=2.71F_d$ | $L/D=2.52F_d$ |

As shown in Table 1, all the turbulence models have a smaller value for *L/D* than the experimental data. The cling length value for SST k-ω is the smallest one while the other models are close to each other. RNG k-ε is the closest one to experimental result.

Predicting the trajectory of jets is one of the key objectives in jet studies. This is also important in the design procedures for disposal outfalls since it provides the distance from the nozzle to where the jet reaches to water surface. This is critical, especially in regions with shallow water depths where depth is not enough to completely dilute the effluent. The trajectory of two numerical cases, as well as the results of several other studies are shown in the Figure 5. The trajectory results obtained using the k-ε turbulence model category are much more accurate than the SST k-ω model. Except for the SST k-ω model, the results of this study are in better agreement with experimental data than the numerical results of Huai et al. (2010).

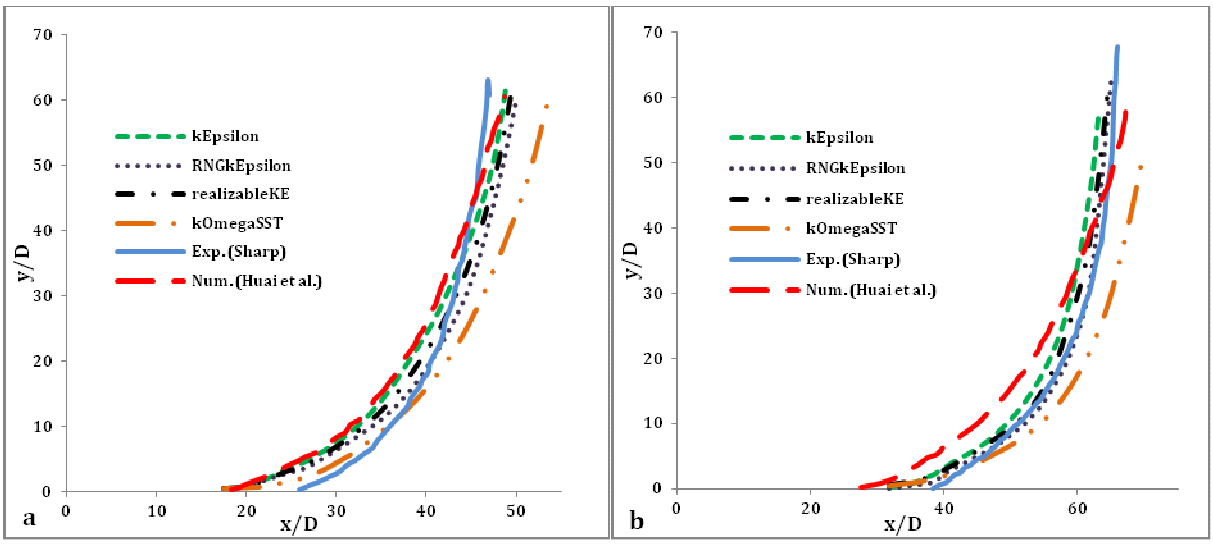

Figure 5: Centerline trajectory. (a) Froude number about 12. (b) Froude number about 20.

### 4.2 Velocity Characteristics

The streamwise (*x*-*y*) velocity profiles along the centerline of the buoyant wall jet were extracted from different simulations. Since each case has four different sub-models itself (four turbulence models for each case), only the results for one case are presented in the following in most figures for brevity. The results of velocity field have been obtained along different jet sections in *x*-direction (different values of *x/D*) at the plane of symmetry. In Figure 6, $U_m$ is the velocity component in the *x* direction (along *y* at central plane), $U_{m0}$ is the maximum of $U_m$ values and its ordinate is *y*. Moreover, $y_{m/2}$ is the velocity-half-height which is the height of $U_m=U_{m0}/2$. On the abscissa and ordinate, $U_{m0}$ and $y_{m/2}$ are taken as the velocity and length scales, respectively. All streamwise velocity profiles show self-similarity and are in good agreement with experimental results by Law and Herlina (2002) as seen in Figure 6. Other previous studies such as Rajaratnam and Pani (1974), Padmanabham and Gowda (1991), and Abrahamsson et al. (1997) are also in agreement with the results showed in the Figure 6. Verhoff's (1963) empirical equation, which is proposed for two-dimensional wall jet, is also in good agreement with the results obtained in the current study. The following equation was suggested by Verhoff:

$$[7] \quad \frac{U_m}{U_{m0}} = 1.48\left(\frac{y}{y_{m/2}}\right)^{1/7}\left[1 - erf\left(0.68\frac{y}{y_{m/2}}\right)\right]$$

From the existing agreement between Verhoff's formula, experimental and present study results, it can be concluded that there is no significant difference in velocity profiles between two-dimensional and three-dimensional wall jets at the symmetry plane (central plane).

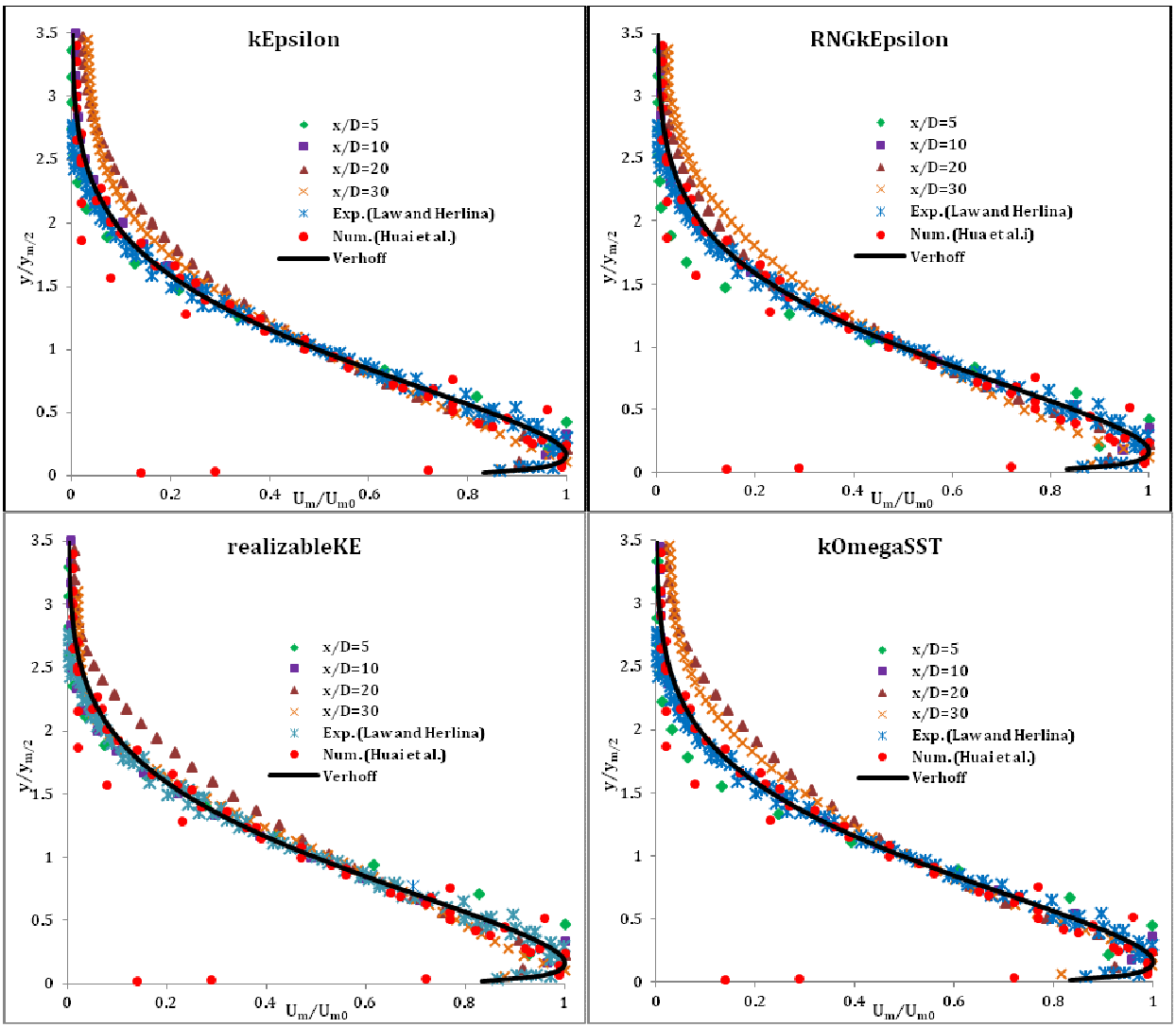

Figure 6: Self similarity of streamwise velocity profiles for different turbulence models.

Among different turbulence models result shown in Figure 6, the results of the SST k-ω model are not as accurate as those of the k-ε category models. On the other hand, RNG and realizable k-ε models results are in better agreement with the experimental data and theory than the results of the standard k-ε model.

### 4.3 Temperature Dilution Characteristics

Dilution is related to the amount of water entrainment achieved by the jet. Dilution is defined as (e.g., Abessi et al., 2010; Huai et al., 2010)

[8] $$S = \frac{T_0 - T_a}{T - T_a}$$

where $T_0$ is the initial jet temperature, $T_a$ is the ambient water temperature, and $T$ is the temperature at the computational mesh. Achieving higher dilution is the main purpose of outfall facilities.
Generally, when the jet is discharged, it behaves like a pure jet (called jet-like flow) for a while and, after passing a transient condition, which is named jet-to-plume-like flow, due to buoyancy forces, it behaves like a pure plume (called plume-like flow). Because of the high momentum force, the dilution in the jet-like

region is less than in the other two regions. Water entrainment reaches the jet centerline at the end of the transient region and a higher dilution rate will subsequently occur.
Figure 7 shows the temperature dilution values along the centerline at the plane of symmetry and at the cross section *y/D=35*. The results are in good agreement with the experimental data of Sharp (1975) for the lower Froude numbers that the experimental data are available for.

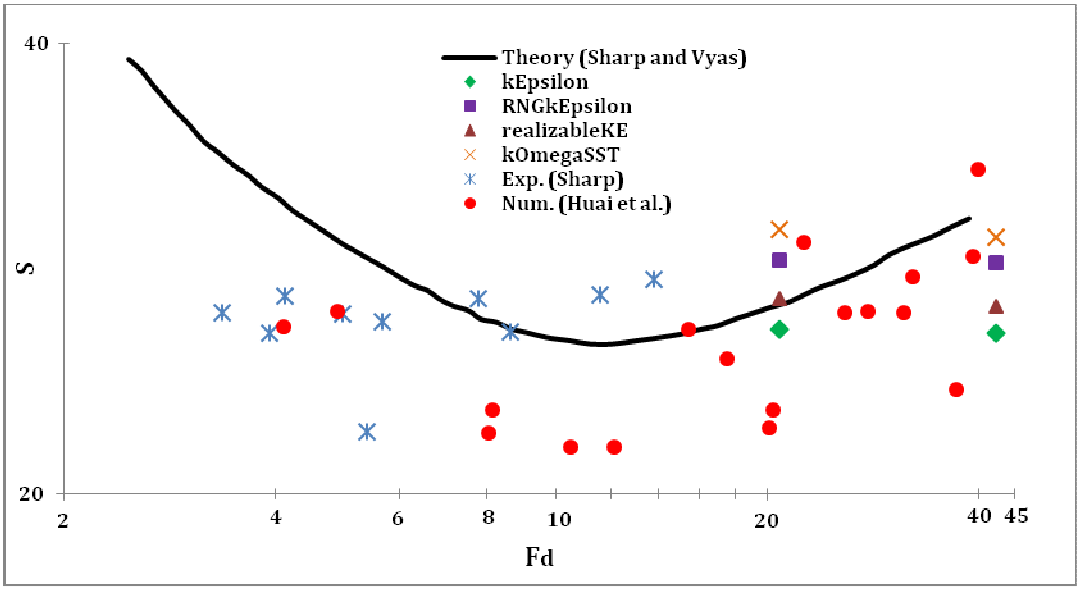

Figure 7: Comparison of temperature dilution at the symmetry plane for different $F_d$ numbers, *y/D=35*.

At lower Froude numbers, the results of realizable k-ε are in good agreement with the theoretical solution proposed by Sharp and Vyas (1977). However, the results of current study underpredict the dilution rate for higher Froude numbers when compared to the results of the theoretical solution. Since experimental data are not available for higher Froude numbers, the numerical results of Huai et al. (2010) are used for comparison in that range. As shown in Figure 7, the numerical results of Huai et al. (2010) are in good agreement with the present study for a Froude number of approximately 40.
Contours of temperature dilutions at the symmetry plane ($z$=0) are plotted in Figure 8 for dilution values of 12, 15, 20, 30, and 60. The most inner layer represents S=12 and the most outer layer corresponds to S=60. Figure 8 shows that the dilution increases with the distance from the source and it depends on both the source (such as the inlet diameter $D$, densimetric Froude number $F_d$, etc), and the ambient water (such as the ambient water depth $H_a$, etc) characteristics. It can be inferred from Figures 7 and 8 that the distance from the discharge source is more important in achieving higher dilution than Froude number.

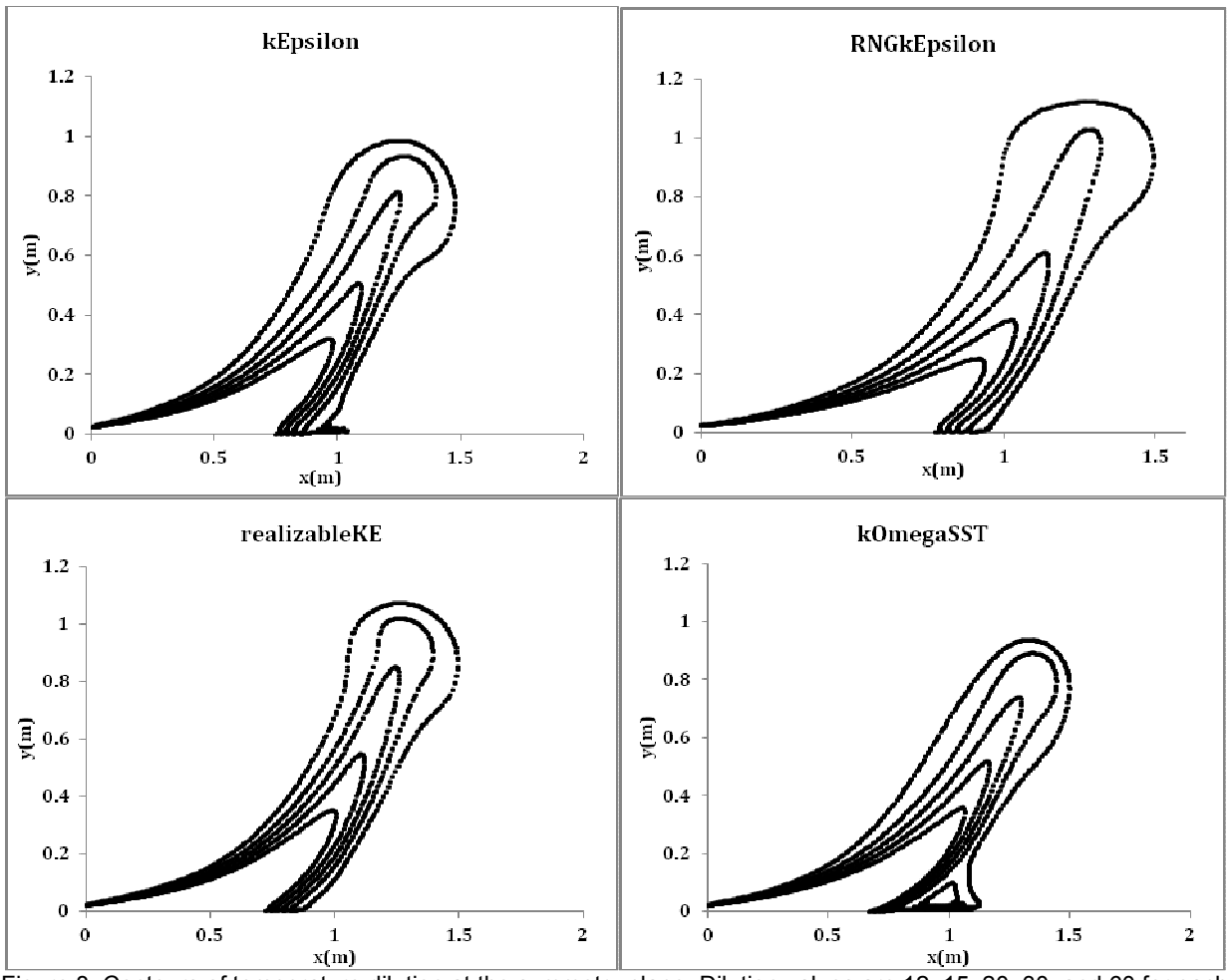

Figure 8: Contours of temperature dilution at the symmetry plane. Dilution values are 12, 15, 20, 30, and 60 for each turbulence model.

## 5 Conclusions

A detailed numerical study was conducted to investigate both velocity and temperature fields of a three dimensional thermal wall jet. Heated water resulted from cooling systems of MSF desalination and power plants is an example of thermal wall jet. Four different turbulence models were applied in order to evaluate the accuracy of RANS models for simulating the discharge of thermal disposals. The numerical results were compared to previous experimental and numerical investigations. The results showed a good agreement with the recent experimental data for velocity and temperature fields. Streamwise profiles for velocity showed self-similarity after an initial distance from discharge point. The general shape of these profiles was also found to be independent of Froude number. Dilution rates for temperature were highly accurate compared to experimental data. However, some discrepancies are observed which could be due to the presence of secondary flows which are not well captured by the turbulence models considered in this study. More advanced turbulence models are expected to improve the accuracy of the simulations for velocity and concentration which is currently in progress by the authors. Finally, among the four models examined in this study, realizable k-ε turbulence model was found to be the most accurate and efficient model for numerical modeling of thermal wall jets discharged into stationary ambient water.

## 6 Acknowledgment

This publication was made possible by NPRP grant # 4-935-2-354 from the Qatar National Research Fund (a member of Qatar Foundation). The statements made herein are solely the responsibility of the authors.

## 7 References

Abessi, O., Saeedi, M., Zaker, N. H., and Kheirkhah Gildeh, H. 2010. Waste field characteristics, ultimate mixing and dilution in surface discharge of dense jets into stagnant water bodies. (in Persian) *J. Water and Wastewater, Vol. 1*.

Abrahamsson, H., Johansson, B., and Lofdahl L. 1997. Turbulence field of a fully develop three dimensional wall jet. *Internal Rep. No. 97/1*, Department of Thermo and Fluid Dynamics, Chalmers Univ. of Tech., Goteborg, Sweden.

Anwar, H. O. 1969. Behavior of buoyant jet in calm fluid. *J. Hydraul. Div., 95.1289-1303*.

Balasubramanian, V., and Jain, S. C. 1978. Horizontal buoyant jets in quiescent shallow water. *J. Environ. Eng. Div., 104(4): 717-730*.

Foster, K., and Parker, G. 1970. Fluids. *Wiley-Interscience*, New York.

Huai, W., Li, Z., Qian, Z., Zeng, Y., and Han, J. 2010. Numerical simulation of horizontal buoyant wall jet. *J. Hydrodynamics, 22(1):58-65*.

Kim, D. G., and Cho, H. Y. 2006. Modeling the buoyant flow of heated water discharged from surface and submerged side outfalls in shallow and keep water with a cross flow. *J. of Environ. Fluid Mech., 6:501-518*.

Kuang, C. P., and Lee, J. H. W. 2002. Effect of control on stability and mixing of vertical plane buoyant jet in confined depth. *J. of Hydraul. Research, 39(4): 375-391*.

Law, A. W., and Herlina. 2002. An experimental study on turbulent circular wall jets. *J. Hydraul. Eng., 128(2): 161-174*.

Maele, K. V., and Merci, B. 2006. Application of two buoyancy-modified k-ε turbulence models to different types of buoyant plumes. *Fire Safety J., 41:122-138.*

Michas, S. N., and Papanicolaou, P. N. 2009. Horizontal round heated jets into calm uniform ambient. *Desalination, 248:803-815*.

OpenCFD Limited. 2011. OpenFOAM - Programmer's Guide, Version 2.1.1.

Padmanabham, G., and Gowda, B. H. .L. 1991. Mean and turbulence characteristics of a class of three dimensional wall jets-Part1: Mean flow characteristics., *J. Fluids Eng., 113:620-628*.

Rajaratnam, N., and Pani, B. S. 1974. Three dimensional turbulent wall jets. *J. of Hydraul. Div., 100(1):69-83*.

Sforza, P. M., and Herbst, G. 1970. A study of three-dimensional incompressible turbulent wall jets. *AIAA J, 8(2):276-283*.

Sharp, J. J. 1975. The use of a buoyant wall jet to improve the dilution of a submerged outfall. *Proc. Instn. Civ. Engrs, Part 2, 59: 527-534*, London, UK.

Sharp, J. J., and Vyas, B. D. 1977. The buoyant wall jet. *Proc. Instn. Civ. Engrs, Part 2, 63: 593-611*, London, UK.

Sobey, R. J., Keane, R. D., and Johnston, A. J. 1988. Horizontal round buoyant jet in shallow water. *J. Hydraul. Eng., 114(8): 910-929*.

Verhoff, A. 1963. The two-dimensional turbulent wall jet with and without an external stream. *Rep. No. 626, Princeton Univ., Princeton, N.J*.

Xiao, J., Travis, J. R., and Breitung, W. 2009. Non-Boussinesq integral model for horizontal turbulent buoyant round jets. *J. Sci. and Tech. Nuclear Installations, 862934*.